

Synthesis and characterization of $\text{BaTiO}_3/\text{CoFe}_2\text{O}_4$ bulk magneto-electric composite system

A Project Thesis Submitted
as a part of the requirements for the degree of

MASTER OF SCIENCE

By

Abhinav Kumar

(PH13M1001)

Under the supervision of

Dr. Saket Ashtana



भारतीय प्रौद्योगिकी संस्थान हैदराबाद
Indian Institute of Technology Hyderabad

DEPARTMENT OF PHYSICS

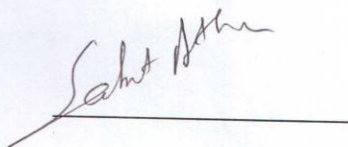
INDIAN INSTITUTE OF TECHNOLOGY HYDERABAD, TELANGANA, INDIA

APRIL, 2015

Declaration

I hereby declare that the matter embodied in this report is the result of investigation carried out by me in the Department of Physics, Indian Institute of Technology Hyderabad under the supervision of Dr. Saket Asthana.

In keeping with general practice of reporting scientific observations, due acknowledgement has been made wherever the work described is based on the findings of other investigators.



Signature of the Supervisor

Dr. Saket Asthana,
Advanced Functional Materials Laboratory,
Department of Physics, IIT, Hyderabad

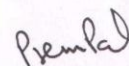


Name of the student – Abhinav Kumar

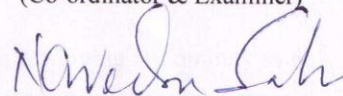
Roll No- PH13M1001

Approval Sheet

This thesis entitled “**Synthesis and characterization of BaTiO₃/CoFe₂O₄ bulk magneto-electric composite system**” by **Abhinav Kumar** is approved for the degree of Master of Science from IIT Hyderabad.



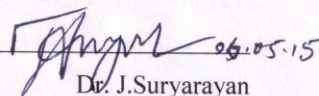
Dr. Prem Pal
(Co-ordinator & Examiner)



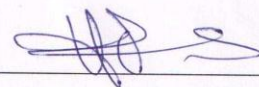
Dr. Narendra Sahu
Examiner



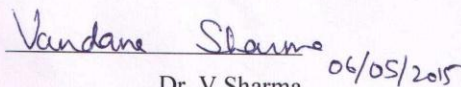
Dr. Jyoti Mohanty
Examiner

 06.05.15

Dr. J. Suryarayan
Examiner



Dr. S. Hundi
Examiner

 06/05/2015

Dr. V. Sharma
Examiner

Acknowledgment

I would like express my high regard to my guide Dr.Saket Asthana for giving oppoutnuty to do work in his “Advance Function Materials Laboratory” , unflinching support & constant visit whilst I set about the project. I am ever so thankful to you sir for your co-operation & suggestions without which this project would not have seen the light of day.

A warm thank you to all the research scholars especially Dr. Durgarav Mr. T. Karthik, Mr. Madhav, Mr Manmohan , Kumar Raja,,Gangaprasad, all of whom support me during the course of my project in different capacities as both mentors & providers.

Last, but not the least, my sincere affection to all my friends, Soumita , Animesh, Ramchandrappa, Parswa,Rajesh and Ravi for giving me company while I toiled hard.

Abhinav Kuamr

Contents	Pages
Abstract	6
1. Introduction	7-15
1.1 Single phase material-	8- 9
1.2 Composite	9
1.3 Why BT and CFO?	9-10
1.4 Structure of Cobalt Ferrite	10-12
1.5 Saturation Magnetic moment in inverse Spinel Structure	12
1.6 Structure of Barium Titanate	12-15
2. Experimental Details	15-19
2.1 Synthesis of Barium Titanate	15-16
2.2 Synthesis of Cobalt Ferrite	16-17
2.3 Formation composite BT-CFO	17
• Flow chart for synthesizing CFO and BT	18
• Flow chart for synthesizing Composite of BT - CFO	19
3. Results and Discussions	20-29
3.1 XRD for CFO	20-22
3.2 M H curve of CFO-	22-23
3.3 Raman Spectroscopy for CFO	23-24
3.4 XRD for BT	4-26
3.5 P-E for BT	26-27
3.5 Raman Spectroscopy for BT	27-28
3.6 XRD for Composite BT-CFO	28-29
4. Future work	29
References	30-31

Abstract

BaTiO₃ (BT), and CoFe₂O₄ (CFO) are well known ferroelectric material and ferromagnetic material respectively which can be prepared by using solid state sintering method and characterized for their ferroelectric and ferromagnetic hysteresis loops and for confirming phase X-ray diffraction and Raman spectroscopy individually are done . . For preparing multi ferroic composites Here we take 65 mole percentage of BT and 35 mole percentage of CFO for studying of composite behavior. For confirming each phase of this composite (phase of BT and phase of CFO) did X-ray diffraction.

1 Introduction

Use of magnetic material is continuously increasing with time to time and it has drawn more research interest. Similarly ferroelectric materials are also being used with same interest but both ferroelectric and magnetic materials are driven through strain by magnetic field and electric field respectively. With the development of electronic technology, composite materials have been widely used for electronic devices where higher densities, limited space and multifunction are required. At present time, the ferroelectric–ferromagnetic composite materials were intensively researched for uses: the magnetic–electric sensors in radio-electronics, microwave electronics, optoelectronics and transducers and the compact electrical filters for suppressing electromagnetic interference (EMI). As for the magnetic–electric sensors, high ferroelectric content was necessary for the composite materials with sufficient resistivity to generate magnetoelctric effect So that coupling between magnetic field and electric field on same material with high sensitivity is very essential requirement. This coupling is called magnetoelctric coupling and materials are called multiferroic materials. Multiferroic material having ferroelectric order, ferroelastic order and ferromagnetic order. When magnetic field is applied on multiferroic material, there will be changes in dimension because of magnetostiction which will affect the polarization of material. It can be vice versa also.

Magnetoelectric coupling is two types-

- 1)-Single phase materials
- 2)-Composite

2.4 Single phase material-

There are two kind of single phase material is found-

- 1) Type 1- (ferroelectric and magnetic orders originate from independent phenomena)
- 2) Type 2 (ferroelectricity is directly linked to the magnetic order).

Type -1 multiferroics (e.g. YMnO₃) seldom have both magnetic and ferroelectric ordering temperatures above certain room temperature. The ordering temperatures for ferroelectricity and magnetism are different as the ferroelectric and magnetic moments arise from different phenomenon. This also makes weak coupling between the magnetic property and ferroelectric property of single phase material. The magnetic property developed from an imbalance between electron spin states and spin-orbit coupling. Ferroelectricity can happen due to lone pairs (ordering of polarizable 6s electron pairs), charge ordering (in equivalence of ion sites and bonds) or ion displacements. BiFeO₃ is a commonly studied Type I single phase multiferroic. It is both antiferromagnetic and ferroelectric and it has been shown that the Curie temperature of both the ferroelectric and anti-ferromagnetic phases are above room temperature.[1]

First single phase material was predicted in Cr₂O₃. [2]

Where BiFeO₃ has a large ferroelectric polarization of $90 \mu\text{C}\cdot\text{cm}^{-2}$ [1,3] it is generally considered that BiFeO₃ contain a weak magnetic moment of $0.05 \mu\text{B}/\text{Fe}$ [4-6]. Demonstrated electric-field-control of antiferromagnetic domains in BiFeO₃ through coupling of antiferromagnetic and ferroelectric domains to the underlying ferroelastic domain structure [7]

In type II multiferroics like TbMnO₃, Ca₃CoMnO₆, the ferroelectric polarization directly originates from particular types of collinear magnetic structures or magnetic spiral structures. In both cases, magnetic interactions produce net polarization at low temperatures, which directly

couples the ferroic order parameters. The coupling between the ferroic order parameters has been largely limited to magnetic field control of ferroelectric polarization.

1.2 Composite-

In case of single phase material, magnetoelectric couplings found because of intrinsic behavior of material which is very weak. First single phase material was predicted in Cr_2O_3 but its magnetoelectric coupling was very weak. So there is highly requirement to move on composite material which is made by composition of two different materials (like magnetic material and ferroelectric material) to increase the strength of magnetoelectric coupling on the material.

Magneto electric composites on other hand have large magneto electric coefficients of magnitude of magneto electric voltage coefficients. The composites are made exploiting the product property of materials.

Composite materials are technical materials made from two or more different materials with significantly different physical or chemical properties and which remain separate and distinct on a difference in difference point view within the finished structure.

1.3 Why BT and CFO?

Under this project, we are using barium titanate as ferroelectric property which consist high ferroelectric property. As Lead-based perovskite-type oxide (Lead Zirconate Titanate – PZT) is the most widely used ferroelectric material. The lead-based perovskite ceramics known for having high piezoelectric. Its polarization at room temp is $26 \mu\text{C cm}^{-2}$ and high electro mechanical property, But the lead-based perovskite having quantity 60% to 70% in weight is very toxic for human body [8]. Hence it is promising demand to explore some magnetoelectric coupling with same new materials which should be lead free. Hence barium titanate is one of the most known material which consist having more polarization as well ferroelectric property.

Cobalt ferrite is magnetic material which are being used as magnetic material. Since structure of inverse spinel structure material has been more intensively understood material.

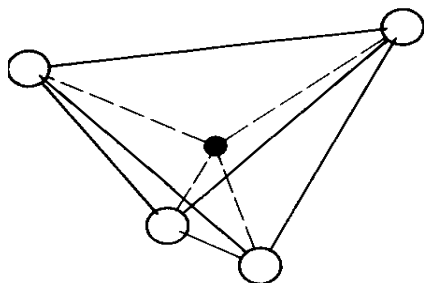
Among spinel structure, Cobalt ferrite is material which consist high magnetostriction property, high chemical stability ,high coercivity moderate saturation magnetization it and mechanical hardness [9] has been reported that linear magnetostrictive strains(λ) up to -252 ppm along with the highest strain derivative $d\lambda/dH$ ($1.33 \times 10^9 \text{ A}^{-1}\text{m}$) under zero applied stress. This strain derivative is found an order of magnitude of terfenol [10-11].

1.4 Structure of Cobalt Ferrite -[12]

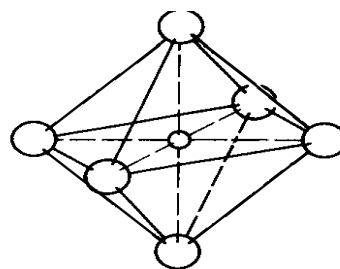
Structure of Cobalt Ferrite is inverse spinel structure. It is called ferrospinel structure because its structure is very closely related to that of mineral structure $\text{MgO} \cdot \text{Al}_2\text{O}_3$. Where M is divalent ion and Al is trivalent ion. Structure is face-centered cubic structure .In one cubic there is found 8 formula unit or total $8 \times 7 = 56$ ions are found in each unit cell.

The large oxygen ions having radius about 0.13 nm are packed quite close together in a face-centered cubic arrangement, and the much smaller metal ions having radii from about 0.07 to 0.08 nm occupy the spaces between them. This space or two types –

- A) -One is called a tetrahedral or A site, because it is located at the center of a tetrahedron whose corners are occupied by oxygen ions.
- B) -Other is called an Octahedral B site metal is placed at center of an octahedral structure whose corner is occupied by six oxygen.



Tetrahedral site



Octahedral site

Figure -1

Environment of both site A and B are different because of two it surrounded by oxygen with two different ways.

If we are considering an unit cell which divided by $a/2$ along the corner of one unit cubic structure thus we can suppose in one cubic cell there are eight octants is found.

Let considering four bellow, the contents of the two lower-left octants are shown in bellow figure(fig 2). One octahedral site occur at center at right octant of figure one is connected by dashed lines to six oxygen ions, two of which, shown dotted, are in adjacent octants behind and below. The oxygen ions are arranged in the same way in tetrahedral in all octants.

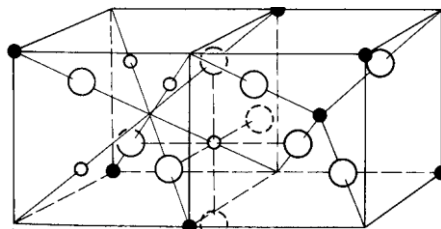


Figure -2: Crystal Structure of cubic ferrite

In this way only, not all the site are occupied by metal ion and Only one-eighth of the A sites and one-half of the B sites are occupied by metals. Since in one cubic cell, there is found 64 tetrahedral and 32 octahedral structure. Thus eight metals occupy on tetrahedral site and 16 metal ion occupy at Octahedral site.

If structure is normal spinel structure, then eight divalent ion will situate at A site (tetrahedral structure) and trivalent ion situate at B site (octahedral structure).

In inverse spinel structure, trivalent occupy it A side and trivalent and divalent occupy B site. In case of cobalt ferrite, whose structure is inverse spinel structure, 8 Fe^{3+} will be placed at tetrahedral structure and 8 Fe^{2+} and 8 Co^{2+} will be situated at octahedral structure.

Site	Number of Available	Number Occupied	Occupants
Tetrahedral structure	64	8	8 Fe^{3+}
Octahedral Structure	32	16	8 Fe^{3+} and 8 Co^{2+}

Table -1

1.5 Saturation Magnetic moment in inverse Spinel Structure, [12]-

Since magnetic moment of oxygen absolute temperature is zero .So that Oxygen does not participate in magnetic moment of spinel structure. In Co^{2+} its consist 3 electrons in 3d orbital thus magnetic moment of Co^{++} is $3\mu\text{B}$ and at Fe^{+3} has 5 electrons in 3d configuration so that magnetic moment in Fe^{+3} is $5\mu\text{B}$. In inverse spinel structure F^{3+} is equally distributed on both the site A and B .Therefore magnetic moment of F^{3+} will be canceled. Thus net magnetic moment of cobalt ferrite will magnetic moment of Co^{2+} which is $3\mu\text{B}$.

Substance	Tetrahedral A site	Octahedral B site	Net magnetic moment
$\text{CoO.Fe}_2\text{O}_3$	Fe^{+3}	Co^{2+} Fe^{3+}	
	5 ↑	3 ↓ 5 ↓	$3\mu\text{B}$ ↓

Table-2

1.5 Structure of Barium Titanate-

Structure of barium titanate is ferroelectric is perovskite which have property of ferroelectric, ferroelastic, piezoelectric and pyroelectric. In perovskite structure ABO_3 shown in figure-3 where B is found in center of unit cell and O is face centered and A is body center of cubic cell. Thus in case of BaTiO_3 , Ba^{2+} will be placed at Corner and Ti^{4+} will placed at the center and O^{2-} will be at center of face in one unit cell.. At room temperature, BaTiO_3 is ferroelectric exhibiting a spontaneous polarization of $26\mu\text{C cm}^{-2}$ [13]. Structure of barium titanate is changing with temperature and ferroelectricity domain with room temperature.

Below its Curie temperature of 120°C , BaTiO_3 is ferroelectric, exhibiting a tetragonal structure at room temperature (Figure- 4). In the tetragonal phase, the polarization will be along the $\langle 001 \rangle$ direction. And extends along the c direction with ratio $c/a = 1.1\%$ displacements are studied.

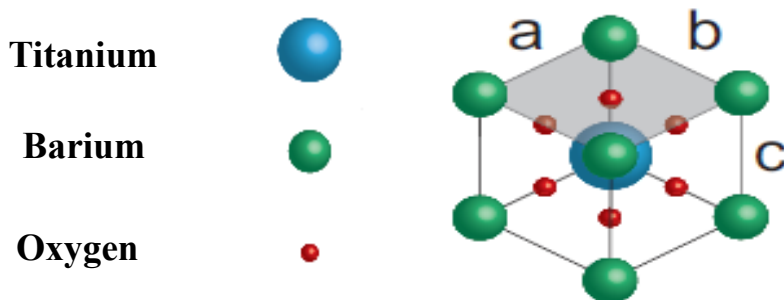


Figure 3: Structure of perovskite structure of Barium Titanate

In this case, the electric dipole moment of the BaTiO_3 unit cell is because of a slight displacements of the O^{2-} ions with respect to the Ba^{2+} and Ti^{4+} ions. The displacements can be seen in the top-view of the tetragonal phase in Figure 5, where the Ti^{4+} ion is moving in the negative y-direction and the O^{2-} ions are moving along the x-axis in the positive y-direction. In this way, small displacement of ion bringing net spontaneous polarization.

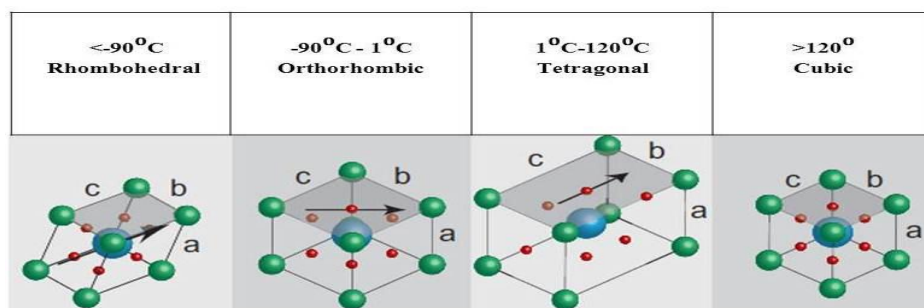


Figure 4: Unit cell of Barium Titanate changing phase with temperature

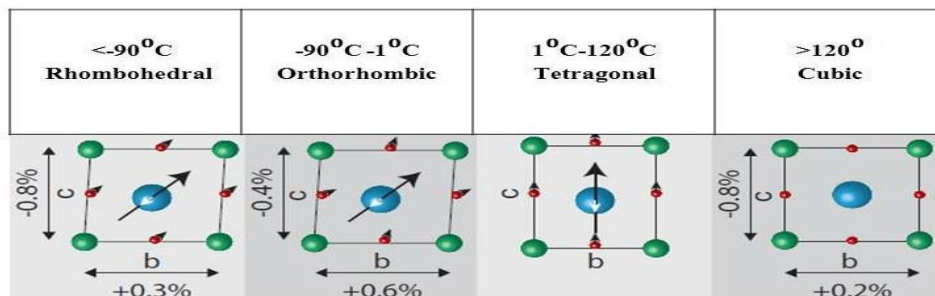


Figure-5: This is showing top view of small displacement of ion with lattice constant and also showing direction of polarization (arrow)

Above the 120°C , its structure becomes cubic where there is no displacement of ion so that net polarization is zero. When cooling through the Curie temperature (120°C), BaTiO_3 cubic structure extends along the c -axis while the a - and b -axes of the unit cell slightly contract. This is a process, which occurs over $\sim -183^{\circ}\text{C}$. At 27°C the lattice elongation of BaTiO_3 amounts to 1.1% [14].

At 1°C temperature, BaTiO_3 undergoes a second phase transition in which tetragonal converts into orthorhombic. As a result of this phase transition the ferroelectric polarization aligns from $\langle 001 \rangle$ to $\langle 011 \rangle$ [15]. On looking top of view of orthorhombic, we will find that the O^{2-} ions are moving in the direction of the polarization and are also slightly displaced towards the nearest Ti^{4+} ion. The Ti^{4+} is moving anti-parallel to the polarization and the Ba^{2+} ions continue to take place at the corners of the unit cell. The unit cell is slightly extending in the direction of the polarization ($\alpha = \beta$ but not equal to 90°).

The final phase transition from orthorhombic to rhombohedra occurs at -183°C . At this phase transition the polarization rotates from $\langle 110 \rangle$ to $\langle 111 \rangle$ ($a = b = c = 4.004$) with α not equal to 90° . The O^{2-} ions are displaced in the direction of the polarization, Ba^{2+} and Ti^{4+} ions are displaced anti-parallel.

2. Experimental Details

2.1 Synthesis of Barium Titanate -



BT is synthesized using solid state sintering method in which BaCO₃ (Barium Carbonate) and CaO (Calcium Oxide) raw materials used from Sigma Aldrich with 99% purity. BaCO₃ and CaO are weighted with stoichiometry and mixed in mortar pestle. Mixed raw materials are grounded for three hours with dryly and by isopropyl alcohol (IPA). After getting homogenous mixture, it is calacined at temperature 1000 for 3 hours for removing CO₂. Calacined sample is re-grinded and sent it for ball milling for reducing particle size by using 100 still ball for 5 hours .Ball milling sample is dried. After this, binder addition is done by using 1 % polyvinyl alcohol and glycerol. For characterization of BT sample, taking some .55 g of BT and making 10 mm pallet using 4.5 tone for 1 minute. And this pallet is kept in furnace at 400⁰C for removing binder addition. Pallet is kept again in furnace at 1350⁰C sintering temperature for densification of sample. After this, obtained sample is ready for characterization.

2.2 Synthesis of Cobalt Ferrite



CoFe₂O₄ is prepared through solid state sintering method using CaO and Co₂O₃ raw materials obtained from Signa Aldrich with 99 percentage purity .Co₃O₄ and Fe₂O₃ are weighted with stoichiometry according to given reaction and mixed in mortar pestle .Mixed raw materials are grounded for three hour with dryly and by Isopropyl alcohol (IPA). After

getting uniform mixture, it is calcined 3 hours for removing O_2 . Calcined sample is re-grinded dryly and send it for ball milling for reducing particle size by using 100 still ball for 5 hours. Ball milling sample is dried and getting dry. After this binder addition is done by using 1% polyvinyl alcohol and glycerol. For characterization of CFO sample, taking some 0.2 g of BT and making .6 mm pallet using 2 tones for 1 minute. And this sample is kept in furnace for sintering at temperature $1350^\circ C$.

. After this obtained sample is ready for further characterization.

2.3 Synthesis of Composite material

For making composite of material .taking 65-BT and 35- CFO of Binder addition calcined BT and CFO is mixed and grinding it properly .Making pallet of .6mm pallet having mass .2 g. Pallets are sintered with temp $1390^\circ C$. Sintered pallet is grinded and taken for XRD and other characterization.

Flow chart for synthesizing BT and CFO

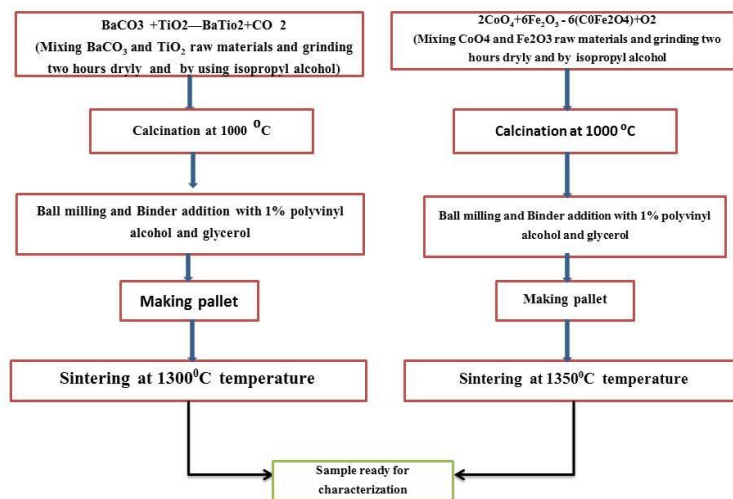


Chart- 1

Flow chart for synthesizing Composite of BT - CFO

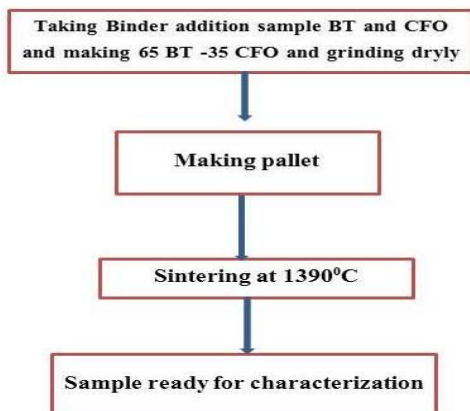


Chart -2

3. Results and Discussions

3.1 XRD for CFO

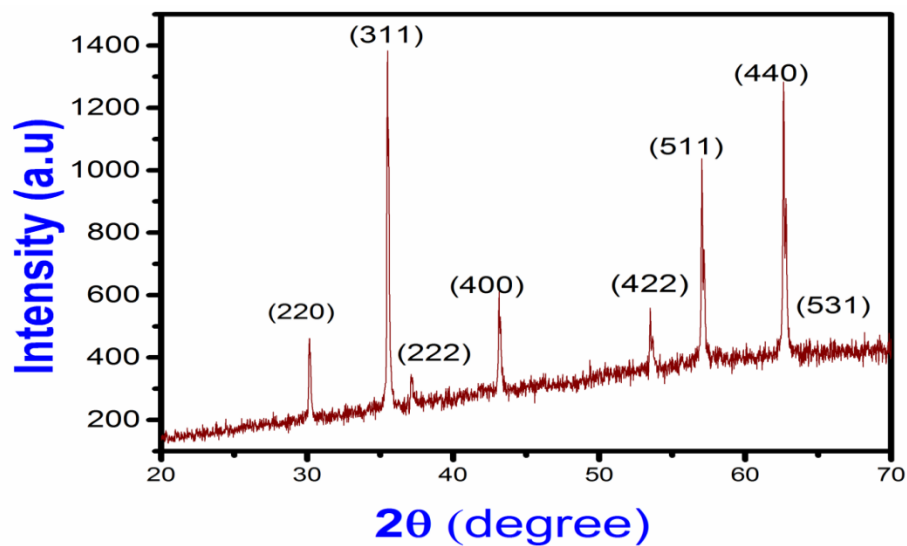


Figure- 6: XRD for CFO at 1300°C

We show the XRD diffraction powder pattern which is synthesized by solid state sintering method at 1300⁰ C sintering temp. XRD pattern is compared with JCPDE file 22-1086 .There is no impurity is detected .It structure is found inverse spinel structure (*Fd3m*) as expecting . Lattice constant is calculated with using Bragg^s diffraction formula which is given bellow and taking index from JCPDF file .

$$2d \sin (2\Theta) =n \lambda$$

$$\text{Where } \frac{a}{\sqrt{h^2+l^2+k^2}}$$

Where, d is interplaner distance

a is lattice constant

h,k and l miller indices

Lattice constant using this formula is calculated 8.3693 Å

The crystallite size is determined by Debye Scherrer formula (Cullity, 1978) using most intense peaks and getting average of them .

$$D = \frac{k\lambda}{\beta(\text{radian}) \cdot \cos(\theta)} \dots\dots\dots (1)$$

$$\text{Where } \beta = \sqrt{\beta_2^2 - \beta_1^2}$$

β_2 = FWHM from Gaussian fitting (degree)

β_1 =0.0008 instrumental error (degree)

where λ (= 1.54056 Å) is the wavelength of k_α X-ray used, θ is the Bragg's angle, β is the full width at half maximum (FWHM) in radian and 'k' is a constant approximately equal to 0.9. In Scherrer's formula, the average crystallite size has been calculated using Gaussian fit, fitted to the peaks in XRD pattern. D has been taken average for all the peaks.

JCPDS(2 θ)	(hkl)	2 θ degree	FWHM(β_2) degree	FWHM(β) degree	Crystalline size(Å)
30.084	(220)	30.1785	0.18368	0.183678258	448.1670616

35.437	(311)	35.5344	0.17273	0.172728147	483.1863062
43.058	(400)	43.1716	0.21797	0.217968532	392.1277695
56.973	(511)	57.0735	0.26296	0.262958783	344.0177277
62.585	(440)	62.6673	0.28116	0.281158862	330.9133155

Table-1

Thus average crystalline size sintered at 1300⁰C sintering temperature is 39.9 nm is found. And lattice constant 8.3693 Å.

3.2 M-H curve of CFO

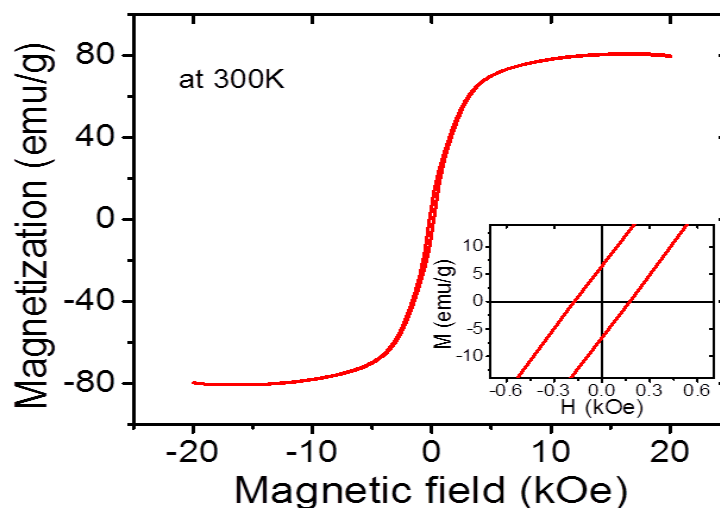


Figure -7 :M-H curve for CFO using VSM

Magnetic characterization of the particles was done using vibrating sample magnetometer (VSM), at room temperature (300K) The M-H curve of CoFe₂O₄ at room temperature gives a picture of ferromagnetic behavior of long range ordering as shown in its sample is sintered at temperature 1300⁰C and crystalline size is calculated 39 nm . And from figure -7 saturation magnetic moment is 81.2 emu /g , correctivity 0.17 kOe and remanent 6.508 emu/g matching with reported value

In ferrite magnetization is function of cation position .Normally in inverse spinel structure cobalt will be situated at B side and Ferrite will be situated at A side .investigated the position of maximum and minimum magnetization moment as function of cation displacement from A site to B site A or vice versa. If there is no cation interchanging then magnetic moment will be minimum.. its mean Cobalt will be placed at B and Iron will be placed A site .

Substance	Saturation magnetization	Coercivity	Remanent
CoFe ₂ O ₃	81.167 emu /g	174.30 Oe	0.508 emu/g

Table 2

3.3 Raman Spectroscopy for CFO

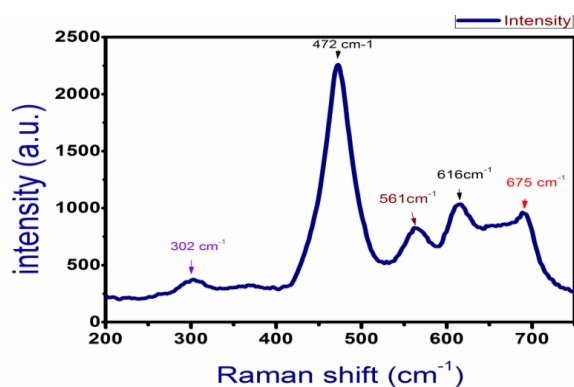


Figure 8 :Raman Spectra for CFO

Raman spectra for the CoFe₂O₄ measured 2.5 mw energy and with wavelength 785 nm and It is found that its structure has inverse spinel structure having space group O_h⁷. In structure half of the Fe³⁺ cations are located on tetrahedral A-site whereas the rest of Fe³⁺ and Co²⁺ cations are distributed over the octahedral B-site+. According to the space group symmetry there should be 39 normal mode A_{1g}+E_g+3F_{2g}+ A_{3u}+4F_u + 2F_{2u} +F_{1g} . In which five Raman active internal modes such as A_{1g}, 1E_g and 3F_{2g} mods are predicted in obedient case. The modes from tetrahedral and octahedral sites can be distinguished by Raman spectroscopy To simplify, peaks

are assigned as for normal spinel structure at presence of five pick show that in agreement with five Raman active mode .But, all five Raman peaks are asymmetric (or dissociated). Assignment of these modes were carried out in accordance with the literature report (Graves et al., 1998). Frequencies above 600 cm^{-1} , i.e., at ion at the 616 and 675 cm^{-1} are due to A_{1g} symmetry involving symmetric stretching of oxygen atom with respect to metal tetrahedral site. The other low frequency phonon modes are due to metal ion involved in octahedral site, i.e., E_g and $3F_{2g}$. These modes correspond to the symmetric and anti-symmetric bending of oxygen atom in M-O bond at octahedral sites.

Sintering Temperature	$A_{1g}(\text{cm}^{-1})$	$A_{1g}(\text{cm}^{-1})$	$F_{2g}(2) (\text{cm}^{-1})$	$F_{2g}(1) (\text{cm}^{-1})$	$E_g (\text{cm}^{-1})$
1300°C	675.9	616.0	472.0	561.0	302

Table 3

3.4 XRD for BT

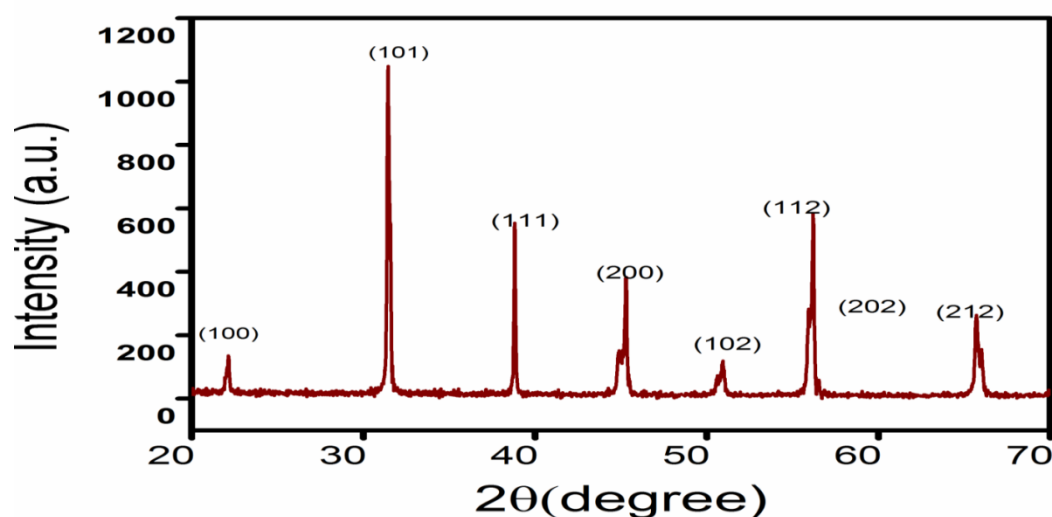


Figure-9 : XRD for BT at 1350°C sintering temperature

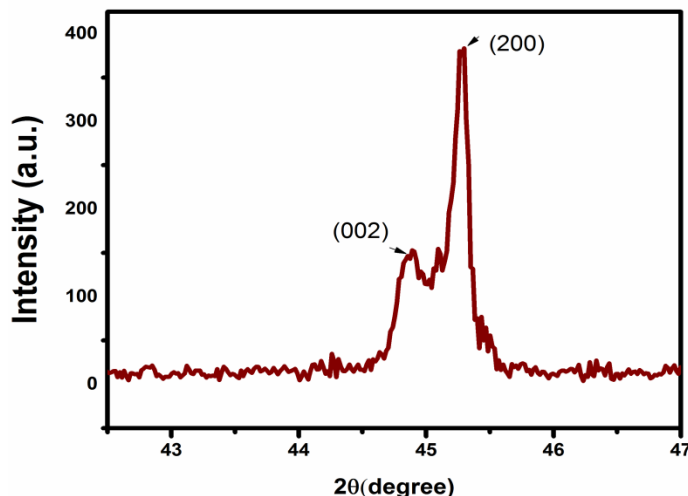


Figure 10: Splitting of (200) pick

A typical XRD pattern of BaTiO₃ bulk particle which is synthesized by solid state sintering method at sintering temperature 1350°C is shown in figure-10. Diffraction peaks of XRD spectra is showing in figure-10 which is matched with cubic Barium Titanate JCPDS no 31-0174 that characteristic of the perovskite structure of a cubic lattice space ($Pm3m$). Using Peaks calculated lattice constant are $a=b=4.020$ nm and $c=4.022$ with $c/a=1$. Using the Scherrer equation (1) for polycrystalline Barium Titanate, determined average crystal size of the BaTiO₃ was 38.2 nm. Due to the small size of the particles composing the the diffraction peaks are broad and it is difficult, from the XRD results alone, to distinguish which of the BaTiO₃ phases (cubic or tetragonal) is dominant. In fact, it is known that for grain sizes below 1 μ m the tetragonal distortion of the barium titanate crystallites is reduced due to the presence of a non-ferroelectric grain boundary layer on the grains surface. However, we observe a broadening of the diffraction (2 0 0) peak in figure 11, it is founding that splitting of (200) is found in (200) and (002) suggesting the stabilization of the polar phase of BaTiO₃.

JCPDS(2 θ)	(hkl)	2 θ degree	FWHM(β) Degree	FWHM(β) Degree	Crystalline size(\AA)
22.001	(100)	22.09326	0.2398	0.239798666	337.7088870
31.387	(101)	31.44945	0.20438	0.204378434	404.0067846

38.776	(111)	38.8036	0.10755	0.107547025	783.5039499
44.964	(200)	45.26134	0.18075	0.180748230	476.3884300
50.626	(102)	50.8495	0.43812	0.438119270	200.8522158
55.910	(112)	56.11405	0.36041	0.360409112	249.8717897
65.501	(202)	65.75544	0.42375	0.423749245	223.3020834

Table 4

3.5 Raman Spectroscopy for BT

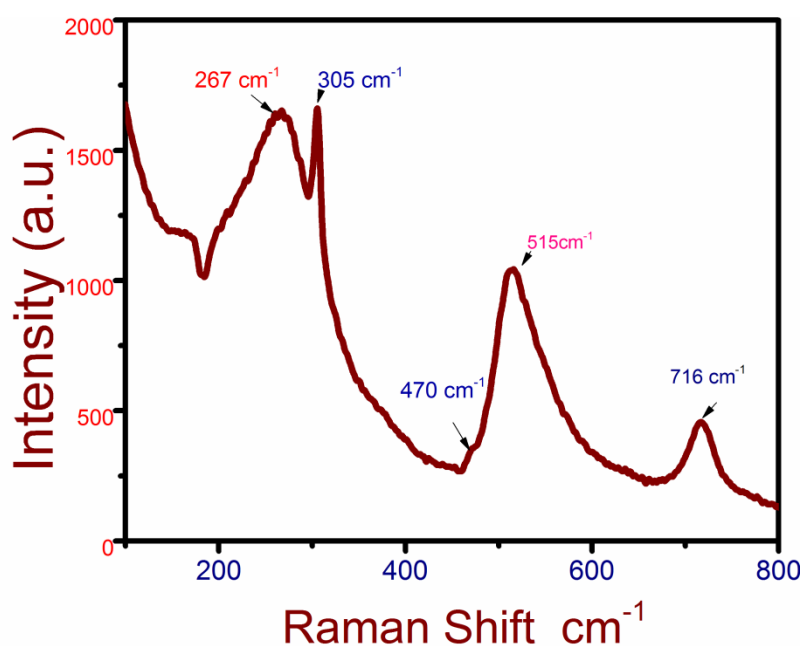


Figure-11 :Raman Spectra for BT

The Raman spectra, for BaTiO₃ ceramic powders samples obtained by solid state route at 1350°C sintering temperature and at room temperature. Since during the continuous heating from -190 to 230 °C, here phase transitions take place: R→O, O→T and T→C. The Raman peaks are shifted and several frequency modes change or disappear as a result of temperature rise. Since in reported paper[15] in case of cubic all picks will disappear almost and in case of rhombohedral

pick corresponding A(TO) will be more sharp and shift toward lower frequency and picks corresponding E(LO),A(TO) will appear but as temperature will increase ,from orthorhombic phase to tetragonal A(TO) and E(LO),A(TO) will disappear and picks will be more broad and pick $B_1, E(TO+LO)$ or 305 cm^{-1} will be more sharp. Thus from above figure 11 pick $B_1, E(TO+LO)$ more sharp which is signifying that BaTiO_3 in tetrahedral phase .

A(TO)	$B_1, E(TO+LO)$	E(LO), A_1 (LO),E(TO)	E(LO),A(TO)	E(LO), A_1 (LO)
267 cm^{-1}	305 cm^{-1}	470 cm^{-1}	515 cm^{-1}	716 cm^{-1}

Table-6

3.6 P -E Curve for BT

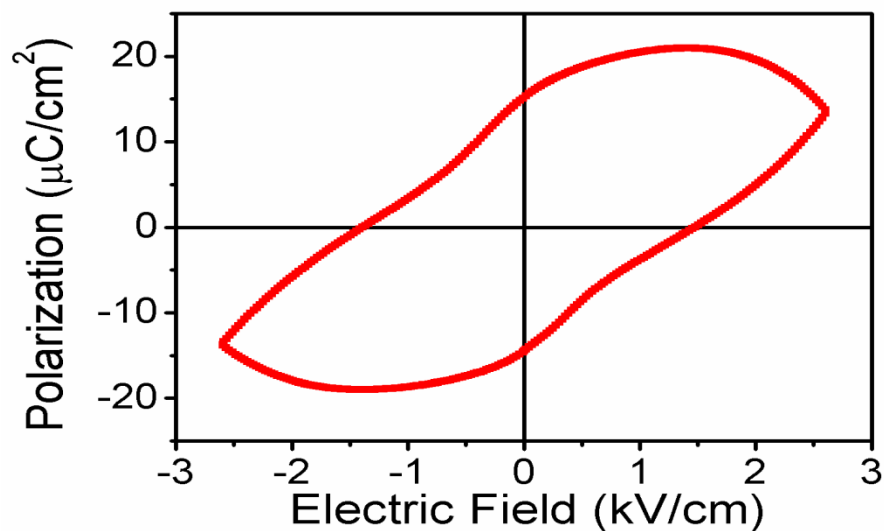


Figure-12:P-E curve for BT

Hysteresis loop	Upward part	Downward part	Average
Remanent polarization(P_r)	$15.6 \mu\text{C cm}^{-2}$	$-14.1 \mu\text{C cm}^{-2}$	$14.85 \mu\text{C cm}^{-2}$
Coercivity (E_c)	$1.49(\text{kV/cm})$	$-1.47(\text{kV/cm})$	$1.47 \mu\text{C (kV/cm)}$

Table 5

Figure 12 shows room temperature P-E hysteresis loop of BT with remanent polarization $P_r=14.85\mu\text{C cm}^{-2}$ at 1350°C sintering temperature. BT is investigated exhibit saturated P-E loop but there some asymmetry is found.

3.6 XRD for BT-CFO Composite

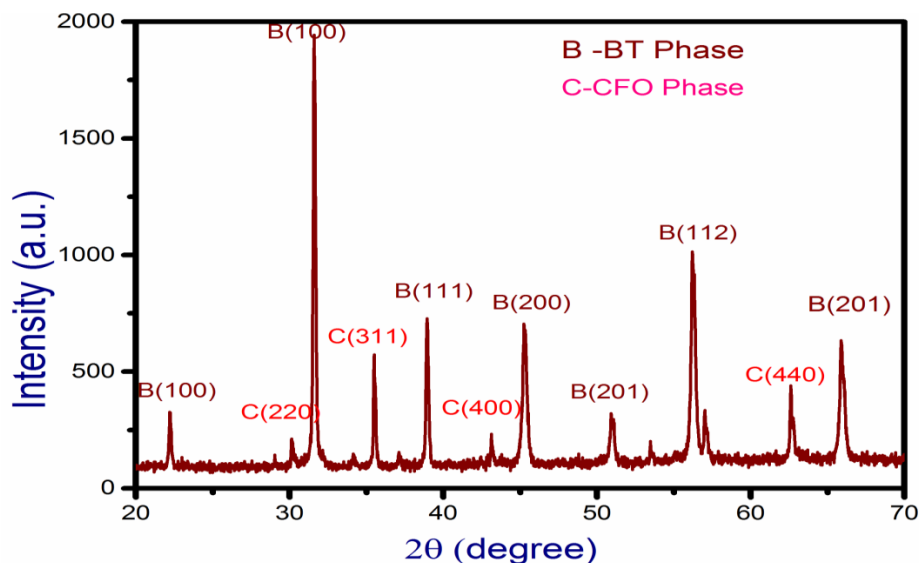


Figure-12: XRD for BT-CFO Composition

From above figure12 X ray diffraction of 60 BT-65 CFO we observe following thing-

- Intensity of barium titanate is higher as comparison to cobalt ferrite phase it will be because of quantity of BT is higher than cobalt ferrite.
- There is some impurity peaks is found which is shown at angle (2θ) 29.03, 43.3 and 57.01 which may be there is some chemical reaction takes place in between BT and CFO.
- In barium titanate seem to be cubic phase because there is no splitting is found of the Bragg reflections corresponding to crystallographic planes (200)/(002) and was observed.

4. Future work

Since in composite material, there is some impurity is found because of chemical reaction in between BT and CFO, so we have to make composite materials which should not have any impurity.

Here we took 65-35 percentage mole of BT-CFO material but apart from this, we can take composite of 50-50, 70-30, 80-20 and 70-30 BT –CFO percentage for studying comparative behavior of composite materials.

In future following work can be done for enhancing the project-

- We have to be sure that there is no phase impurity.
- We can measure magnetostiction for composite as well individually material.
- M -H and P-E curve can be measured for study magnetic and ferroelectric behavior

- Optimization of the composition for the highest magnetoelectric voltage co-efficient

References

[1] J. Wang, J. B. Neaton, H. Zheng, V. Nagarajan, S. B. Ogale, B. Liu, D. Viehland, V. Vaithyanathan, D. G. Schlom, U. V. Waghmare, N. A. Spaldin, K. M. Rabe, M. Wuttig, And R. Ramesh, *Science* 299, 1719 (2003).

[2]. Magnetoelectric Effect In Composite Materials Girish Harshé, Joseph P. Dougherty And Robert E. Newnham Materials Research Laboratory, The Pennsylvania State University
University Park, Pa 16802

[3] J. Dho, X. Qi, H. Kim, J. L. Macmanus-Driscoll, And M. G. Blamire, *Advanced Materials* 18, 1445 (2006).

[4].C. Ederer And N. A. Spaldin, *Physical Review B* 71, 060401 (2005).

- [5] J. B. Neaton, C. Ederer, U. V. Waghmare, N. A. Spaldin, And K. M. Rabe, Physical Review B 71, 014113 (2005).
- [6] H. Bá, M. Bibes, A. Barthélémy, K. Bouzehouane, E. Jacquet, A. Khodan, J.-P. Contour, S. Fusil, F. Wyczisk, A. Forget, D. Lebeugle, D. Colson, And M. Viret, Applied Physics Letters 87, 072508 (2005).
- [7] T. Zhao, A. Scholl, F. Zavaliche, K. Lee, M. Barry, A. Doran, M. P. Cruz, Y. H. Chu, C. Ederer, N. A. Spaldin, R. R. Das, D. M. Kim, S. H. Baek, C. B. Eom, And R. Ramesh, Nature Materials 5, 823 (2006).
- [8] Effect Of CoFe_2O_4 Mole Percentage On Multiferroic And Magnetoelectric Properties Of $\text{Na}_0.5\text{Bi}_0.5\text{TiO}_3/\text{CoFe}_2\text{O}_4$ Particulate Composites R.V. Krishnaiaha, A.Srinivasa,N, S.V.Kamata, T.Karthikb, Saketasthanab
- [9] Spinel Cobalt Ferrite By Complexometric Synthesis Pham D. Thang_, Guus Rijnders, Dave H.A. Blank
- [10] Junyi Zhai, Shuxiang Dong, Zengping Xing, Jiefang Li, D. Viehland, Appl. Phys. Lett. 89 (2006) 083507.
- [11] Y. Chen, J.E. Snyder, K.W. Dennis, R.W. Mccallum, D.C. Jiles, J. Appl. Phys. 87 (2000) 5798.
- [12]- B. D. Cullity, C. D. Graham Introduction To Magnetic Materials 2008 (1) (2)
- [13] C. Kittel, Reviews Of Modern Physics 21, 541 (1949).
- [14] H. D. Megaw, Proceedings Of The Royal Society Of London. Series A. Mathematical And Physical Sciences 189, 261 (1947).

[15] G. H. Kwei, A. C. Lawson, S. J. L. Billinge, And S. W. Cheong, The Journal Of Physical Chemistry 97, 2368 (1993).

[16] E.V. Mejía-Uriarte*1, R.Y. Sato-Berrú2, M. Navarrete3, O. Kolokoltsev4, J. M. Saniger5